INTERNATIONAL JOURNAL OF INTEGRATED ENGINEERING
ISSN: 2229-838X e-ISSN: 2600-7916

IJIE

Vol. 17 No. 6 (2025) 135-146
https://publisher.uthm.edu.my/ojs/index.php/ijie

On Thin Flexible Wideband Printed Vivaldi Antenna for Sub-6 GHz Wearable Applications

Sadia Afroz[1], Azremi Abdullah Al-Hadi[1]*, Saidatul Norlyana Azemi[1], Wee Fwen Hoon[1], Surentiran Padmanathan[1], Che Muhammad Nor Che Isa[1], Yen San Loh[2], Lun Hao Tung[2], Lai Ming Lim[2], Zambri Samsudin[2], Idris Mansor[2], Ping Jack Soh[3]

[1] *Advanced Communication Engineering (ACE) Center of Excellence, Faculty of Electronic Engineering & Technology, Universiti Malaysia Perlis, Perlis, MALAYSIA*
[2] *Manufacturing Technology & Innovation Department, Jabil Circuits Sdn. Bhd., Penang, MALAYSIA*
[3] *Centre for Wireless Communications (CWC), University of Oulu, 90570 Oulu, FINLAND*

*Corresponding Author: azremi@unimap.edu.my
DOI: https://doi.org/10.30880/ijie.2025.17.06.011

Article Info

Received: 17 March 2025
Accepted: 28 October 2025
Available online: 30 December 2025

Keywords

5G applications, antipodal vivaldi, polyimide, polyester, SAR

Abstract

The growing adoption of Body Area Networks (BANs) significantly enhanced the desire of wearable antennas. This study introduces a flexible wearable printed antenna based on an antipodal Vivaldi structure fabricated on a hybrid polyimide-polyester substrate utilizing screen printing fabrication technic, as well as a flexible dual-ring antenna utilizing copper tape and a polyester substrate. Compare to rigid antennas, flexible wearable antennas require meticulous fabrication and measurement processes due to their structural sensitivity. This paper provides a comprehensive analysis on the procedure of fabrication and considerations during measurement of the flexible wearable antennas, alongside a comparative analysis between them. These antennas exhibited satisfactory free-space performance, covering key 5G NR bands, including n48, n77, and n78. Printed antenna demonstrated wider resonance bandwidth oppose to the copper tape antenna and exhibited a higher degree of alignment among simulation and measurement. These findings indicate that the printed antenna offers superior performance and durability. To validate its applicability in wearable scenarios, the printed antenna was assessed under on-body placement and mechanical deformation. On-body measurements were conducted at the chest and back, yielding resonance bandwidths of 710 MHz and 740 MHz, respectively, with good agreement between simulation and measurement. Simulation results under various bending conditions demonstrate that the antenna maintains satisfactory resonance performance compared to its free-space response. At a bending radius of 50 mm, the measured S-parameters closely align with simulation results, exhibiting a resonance bandwidth of 650 MHz. SAR analysis verified that the antenna meets ICNIRP safety standards, confirming its safe operation for wearable use

1. Introduction

Body Area Networks (BANs) are extensively utilized across various domains, including health and sports monitoring, emergency response, and navigation [1]. In BAN communication systems, wearable devices rely on wearable antennas for efficient wireless signal transmission and reception [2]. For comfort of the user and reduced electromagnetic radiation, wearable antennas requires characteristics like lightweight, thin, low-profile and flexibility [3]. Textiles such as polyester, cotton, linen, and denim are commonly used because of lower height and lower dielectric constants [4].

In textile-based antennas with thin substrates, the radiating patch and ground plane are often fabricated utilizing copper tape. A dual-ring circular patch antenna was initially designed using a polyester substrate and copper tape [5]. Although it exhibited satisfactory performance, its bandwidth was limited. To overcome this constraint, Vivaldi structure was chosen because of its excellent ultra-wideband inherent capabilities [6], [7], along with other advantages such as low cost, lightweight structure, and a simple feeding mechanism, makes it suitable for various 5G applications. Furthermore, among different Vivaldi antennas, the antipodal Vivaldi antenna (AVA) is vastly used for broader bandwidth and better performance which is consisting of two symmetrical tapered arms, separated by a slot. However, fabrication using copper tape presents durability concerns, as repeated wear can cause the conductive layer to peel off, compromising efficiency and long-term performance [8]. To address this, screen printing technology was adopted as an alternative fabrication method, offering enhanced mechanical stability and durability. This technique employs a patterned stencil to deposit conductive ink onto the substrate, ensuring better structural integrity over time [9]. A hybrid polyimide–polyester substrate was proposed to further improve robustness compared to polyester alone. Consequently, the screen-printed Vivaldi antenna replaced the copper tape-based design. This study provides a comparative free-space performance analysis between the copper tape-based dual-ring circular patch antenna [5] and the screen-printed antipodal Vivaldi antenna [10], highlighting the improvements achieved through the new design and fabrication approach.

Considering wearable nature of the screen-printed antenna, the outcomes from the antenna near body must be thoroughly examined since wearable antennas operate in close proximity to the human body, their performance tends to degrade, particularly in terms of resonance, efficiency and gain [11]. Human body, acting as a lossy medium, would significantly impact antenna performance, often causing degradation [12]. As a wearable textile antenna, it will inevitably experience bending when positioned on different body areas [13]. Impedance mismatches between the feeding port and the transmission line can be occurred by bending, potentially altering and degrading overall performance. Therefore, ensuring that the antenna maintains stable operation under mechanical deformations caused by moving user is crucial [14]. Wearable devices can lead to high Specific Absorption Rate (SAR) levels at the skin surface [15]. Specific Absorption Rate (SAR) is defined as the power absorbed by the biological tissue when exposed to a RF electromagnetic field [16]. Consequently, assessing SAR value is crucial and the limits were enforced by regulatory agencies (such as the United States and the European Union) in different nations. For instance, the European Union has imposed SAR restrictions of 2 W/kg, averaging over 10 g of tissue. In contrast, the Federal Communications Commission (FCC) has set SAR limits of 1.6 W/kg, averaging over 1 g of tissue for cell phones and similar electronic devices [16], [17], [18], [19].

Screen-printed antennas have been explored in various studies. For instance, a dual-band circularly polarized MIMO wearable antenna was screen-printed on a cotton–polyester fabric for WBAN applications at 2.45 GHz and 5.8 GHz, achieving bandwidths of 400 MHz and 800 MHz, respectively [20]. Another study [21] employed screen-printed antennas on polyimide, glass, and alumina ribbon ceramic substrates, operating at 24 GHz. Additionally, an ultra-wideband screen-printed antenna on a borosilicate glass substrate demonstrated a bandwidth ranging from 7.92 GHz to 36.5 GHz [22]. In contrast, the proposed printed antenna employs a dual-layer substrate comprising polyester and polyimide to balance user comfort and mechanical stability, targeting sub-6 GHz frequencies for 5G applications.

Considering the factors described earlier, in response to these challenges, this study illustrates analysis of fabrication process, measurement concerns, along with performance evaluation in both free-space and wearable conditions, including proximity to the human body and structural deformation due to bending. SAR analysis has been performed to ensure safety of user. Structure of the paper follows: Section 2 presents the antenna design, fabrication process, and measurement setup. Results and key findings are discussed in Section 3, while Section 4 summaries the study.

2. Design Specifications, Fabrication, and Performance Analysis Setups

2.1 Design Specifications

Figure 1 portrays a dual-ring circular patch and fabricated was done with a polyester textile whose dielectric constant is 1.34 with loss tangent value of 0.005, along with the height of 0.4 mm. In contrast, printed antenna comprises of two-layered combined substrate consisting of polyimide (dielectric constant: 2.1, loss tangent: 0.0015, height: 0.05 mm) and polyester, illustrated in Figure 2. The conductive elements of the circular patch and

Int. Journal of Integrated Engineering Vol. 17 No. 6 (2025) p. 135-146

antipodal Vivaldi antennas are realized using copper tape and silver ink, respectively. Detailed values for dimensions of both antennas are presented in Tables 1 and 2. Further enhancement of bandwidth is done by selecting antipodal Vivaldi structure for printed antenna as an improvement over the previously used dual-ring circular patch configuration.

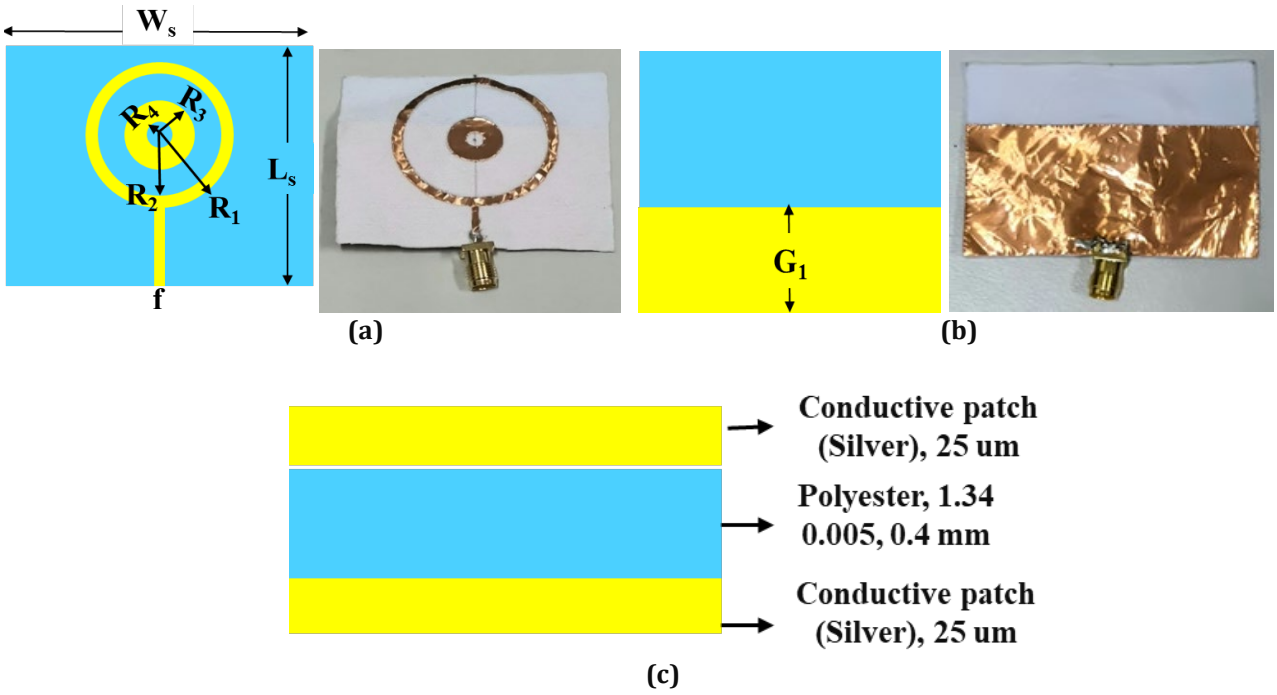

Fig. 1 *Dual-ring circular patch antenna with copper tape (a) front (simulated and fabricated); (b) rear (simulated and fabricated); (c) simulated side view*

Table 1 *Parameters of dual-ring circular patch antenna*

Parameters	Description	Value (mm)	Parameter	Description	Value (mm)
W	Antenna width	55	f	Feedline width	1.3
L	Antenna length	46	G	Ground width	33
R1	Outer radius of outer circle	17	R3	Outer radius of inner circle	5.5
R2	Inner radius of outer circle	15	R4	Inner radius of inner circle	2

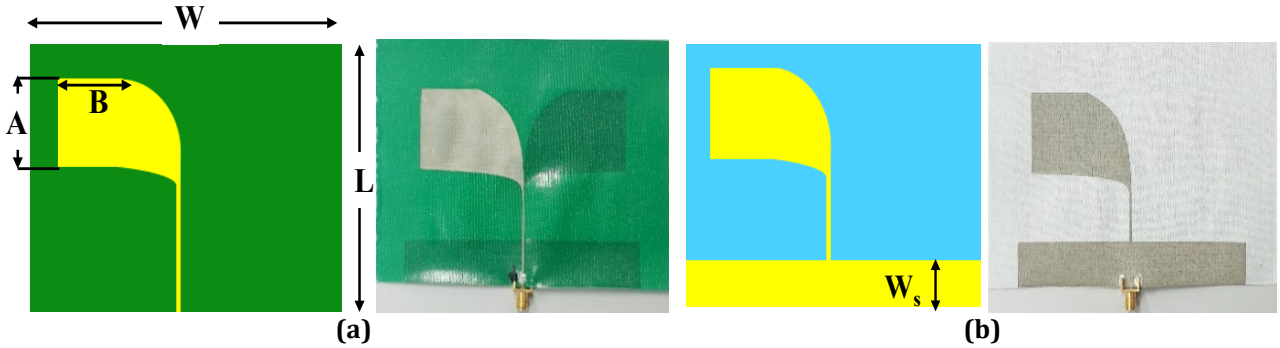

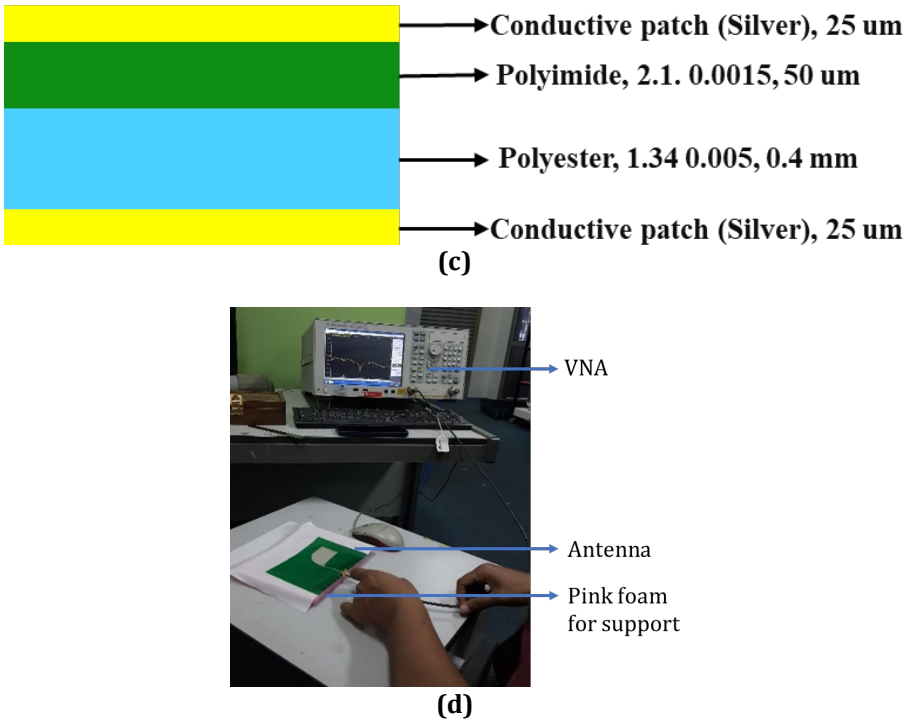

Fig. 2 *Antipodal Vivaldi antenna (a) front (simulated and fabricated); (b) back (simulated and fabricated); (c) simulated side view; (d) measurement setup*

Table 2 *Parameters of antipodal Vivaldi antenna*

Parameter	Description	Value (mm)
W	Antenna width	120
L	Antenna length	95
A	Flare length	36
B	Flare width	28
Ws	Ground width	20

2.2 Procedure for Fabrication and Concerns for Measurement

2.2.1 Dual-Ring Circular Patch Antenna

Fabrication of the dual-ring circular patch antenna start with manually cutting copper tape and polyester following predefined layers in simulation (radiating patch, and substrate). Conductive elements were then positioned onto the substrate, and 50 Ω SMA connector attachment to feedline is achieved through conventional lead soldering. Prior to measurement, the connection of the antenna feedline and SMA was checked using with the help of multi-meter. Figure 1(a) and 1(b) illustrates fabricated antenna.

2.2.2 Antipodal Vivaldi Antenna

Fabrication of antipodal Vivaldi antenna was conducted using a screen-printing process and the process is portrayed in Figure 3. Initially, a polyimide substrate was pre-laminated on polyester utilizing a heat press laminator. Conductive elements, including the radiating patch and ground plane, were then went to screen printing in several layers using silver ink. For silver conductive ground layer and silver conductive patch antenna layer, 25µm thickness of screen-printed silver ink was printed using 230 thread/inch meshes. Attachment of 50 Ω SMA connector with feedline was achieved utilizing silver soldering paste and the process is shown in Figure 3(d). Traditional soldering methods were avoided, as they could potentially damage or burn the polyimide layer. Instead, soldering paste was precisely applied using a syringe to ensure accuracy. The antenna was subsequently put in the oven with temperature of 100°C for approximately 45 minutes for making this silver paste into solid,

Int. Journal of Integrated Engineering Vol. 17 No. 6 (2025) p. 135-146

ensuring proper connection among SMA connector and antenna. Fabricated antipodal Vivaldi antenna is shown in Figure 2(a) and 2(b). Entire procedure of printing was conducted using an automated printer, followed by curing in a convection oven. All fabrication procedures were performed at the MTI Lab, Jabil Circuits, Penang.

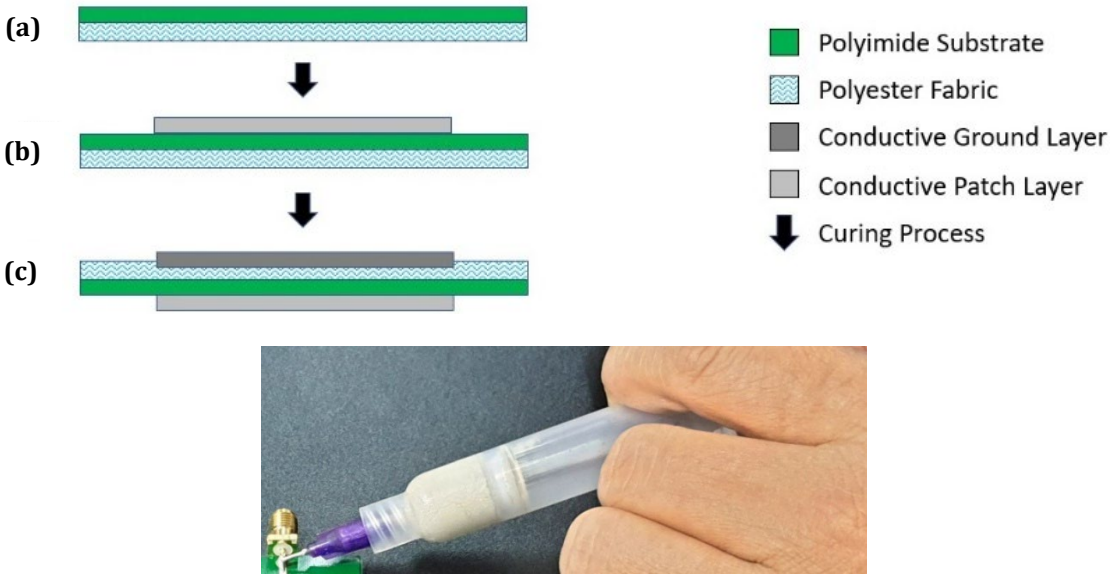

Fig. 3 *Antipodal Vivaldi antenna fabrication procedure (a) polyimide substrate heat press on polyester fabric; (b) conductive patch layer screen printed on the top; (c) flip the substrate and screen print on the conductive ground layer; (d) SMA attachment utilizing silver ink using syringe for precision*

Table 3 *Difference between two antennas in term of fabrication*

Dual-ring circular patch antenna	Antipodal Vivaldi antenna
Placing copper tape	Using screen printing technic
Easy and less time-consuming fabrication	Fabrication is time-consuming and requires to follow in steps
Copper may detach on multiple use	Printed silver conductive, No possibility of detachment
Not long-lasting	Durable
Cheaper	Comparatively expensive
Mild error in outcomes due to manually done fabrication	Using machinery, more precious structure

Table 3 presents a comparative analysis, highlighting that while copper tape enables a faster, simpler, and more cost-effective fabrication process, it lacks long-term durability. In contrast, printed antennas demonstrate superior resilience, allowing for repeated use without performance degradation. Furthermore, printed structures are more accurate than manually fabricated dual-ring antenna, leading to increased accuracy in measurement results. Afterward, as shown in Figure 2(d), reflection coefficient measurements were performed utilizing Vector Network Analyzer (VNA), model E5071C. While measuring these single-port antenna, either of the two available ports utilized for connection purpose with antenna, and corresponding result can be seen on the screen. Sustaining the wearability of the antenna and its thin, flexible substrate, precise measurement was crucial. To ensure stability while maintaining free-space conditions, a foam backing is placed to rear side of the antenna while measuring. The dielectric properties of the foam closely resemble those of air, providing structural support without significantly affecting the antenna's electromagnetic characteristics.

2.3 On-Body Setup of Antipodal Vivaldi Antenna

To assess impact on antenna performances due to human body, a realistic homogeneous human body model from CST Microwave Studio was employed in simulation, as it accurately replicates the electromagnetic properties of human body. Antenna positioning has been done at two distinct locations: the chest and back to analyse its

resonance characteristics, as illustrated in Figures 4 and 5. The placement was as close as possible to the body, with a minimum separation of 5.6 mm, constrained by the SMA connector and the antenna structure.
To experimentally validate the simulation results, the antenna's performance was tested on a real human subject under similar conditions. The 5.6 mm separation was maintained by placing a foam layer (height: 5 mm) on back of the antenna, Considering the thickness of a typical T-shirt worn by the human model, the effective separation was approximately 5.6 mm. Consequently, consistency between the simulation and measurement setups was ensured. The measurement configurations are depicted in Figure 5.

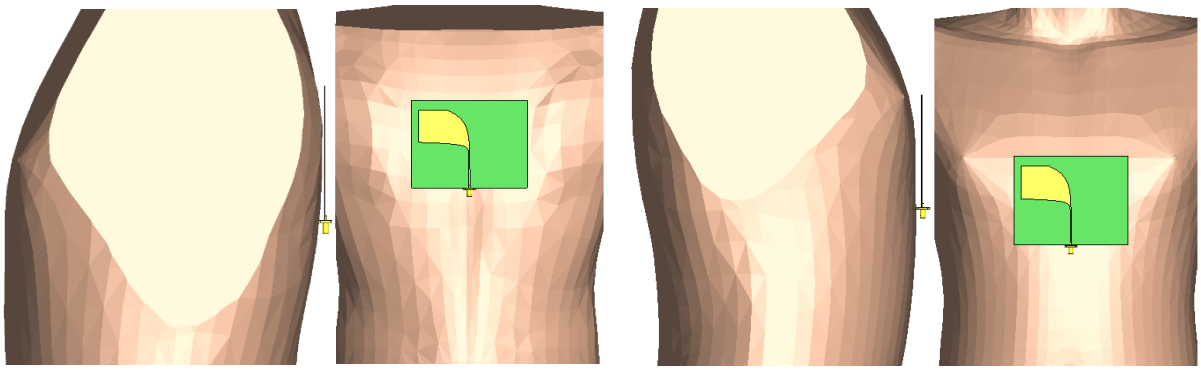

(a) (b)

Fig. 4 *Antipodal Vivaldi antenna placement near human model in CST on the (a) back of the model; (b) chest of the model*

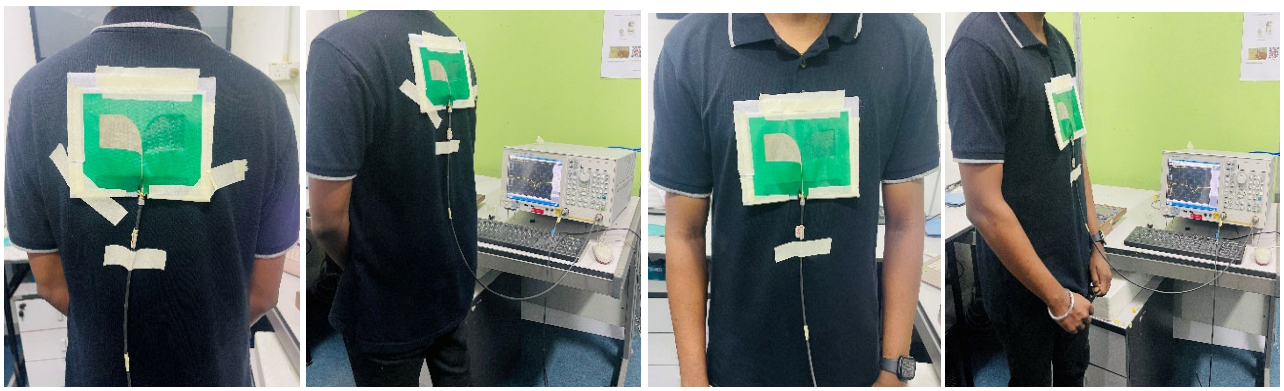

(a) (b)

Fig. 5 *Antipodal Vivaldi Antenna placement near real human body for measurement on (a) back; (b) chest*

2.4 Antipodal Vivaldi Antenna Bending Setups

Since printed antenna is developed for wearability, the antenna requires to maintain its performance under bending conditions, since antenna would inevitably go through deformation like bending when user wears it. Figures 6 along with 7 illustrate the simulation and measured setup of bending analysis, respectively for printed antenna. To simulate bending, antenna is wrapped around a cylinder for which vacuum is chosen as material, assuring cylinder property would not interfere with its electromagnetic properties. The degree of bending is controlled by varying the radius of cylinder. Simulations are performed for different cylinder radius for determining impact of bending. To evaluate the outcomes of antenna through experimental measurements, a hollowed cylinder was used instead of a solid rigid structure. This design ensures that the interior of the cylinder remains filled with air, with only the outer surface providing structural support. To further make the cylinder characteristics resembling air/vacuum, air holes were incorporated into the outer surface of the cylinder. The antenna was then placed on cylinders of varying radii to assess its performance under different bending conditions.

Int. Journal of Integrated Engineering Vol. 17 No. 6 (2025) p. 135-146

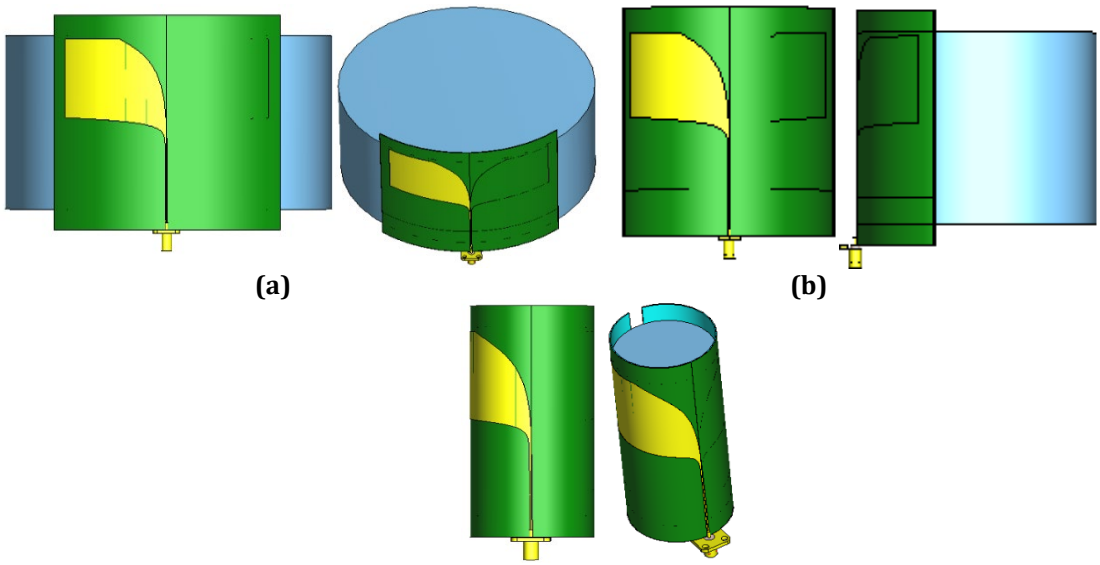

Fig. 6 *Simulated antipodal Vivaldi antenna bended antenna at different bending radius (a) 80mm; (b) 50mm; (c) 20mm*

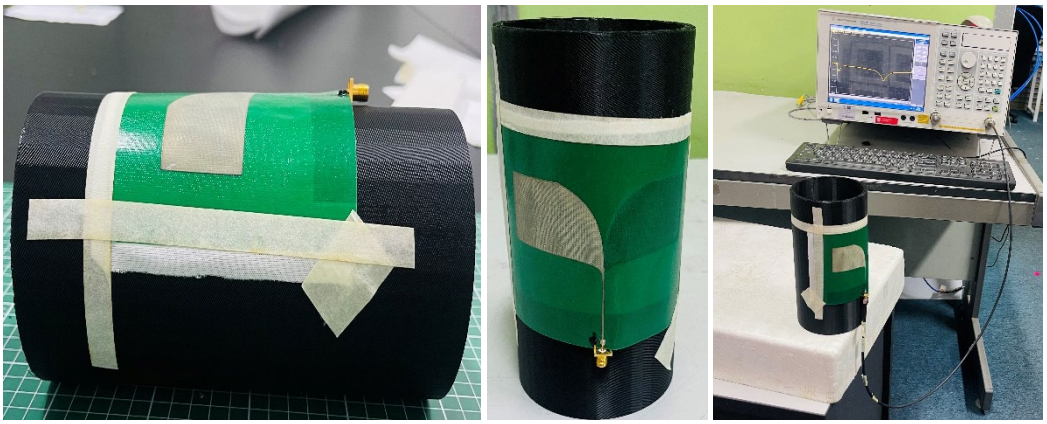

Fig. 7 *Measurement setups for antipodal Vivaldi antenna bending with bending radius 50 mm*

3. Results and Discussions

3.1 Free Space Results of Dual-Ring Circular Patch and Antipodal Vivaldi Antenna

The measurement results demonstrated satisfactory performance, as they closely aligned with the simulation outcomes, as presented in [5], [10]. Through outcomes that demonstrated in Figures 8(a) and 8(b), satisfactory alignment between measurement and simulation is confirmed. Hence, printed antenna exhibits a higher degree of correlation with simulations, highlighting validity of screen-printing fabrication and the tactics that followed during measurement. This finding underscores the suitability of screen-printing technology for fabricating thin, flexible antennas. Furthermore, the printed antenna exhibited improved efficiency and gain compared to its copper tape counterpart, portrayed in Figures 8(c) and 8(d). Since printed antenna exhibits better performance, further assessment i.e. on-body and bending are conducted on the printed antenna only and reassuring the wearable application of the antenna.

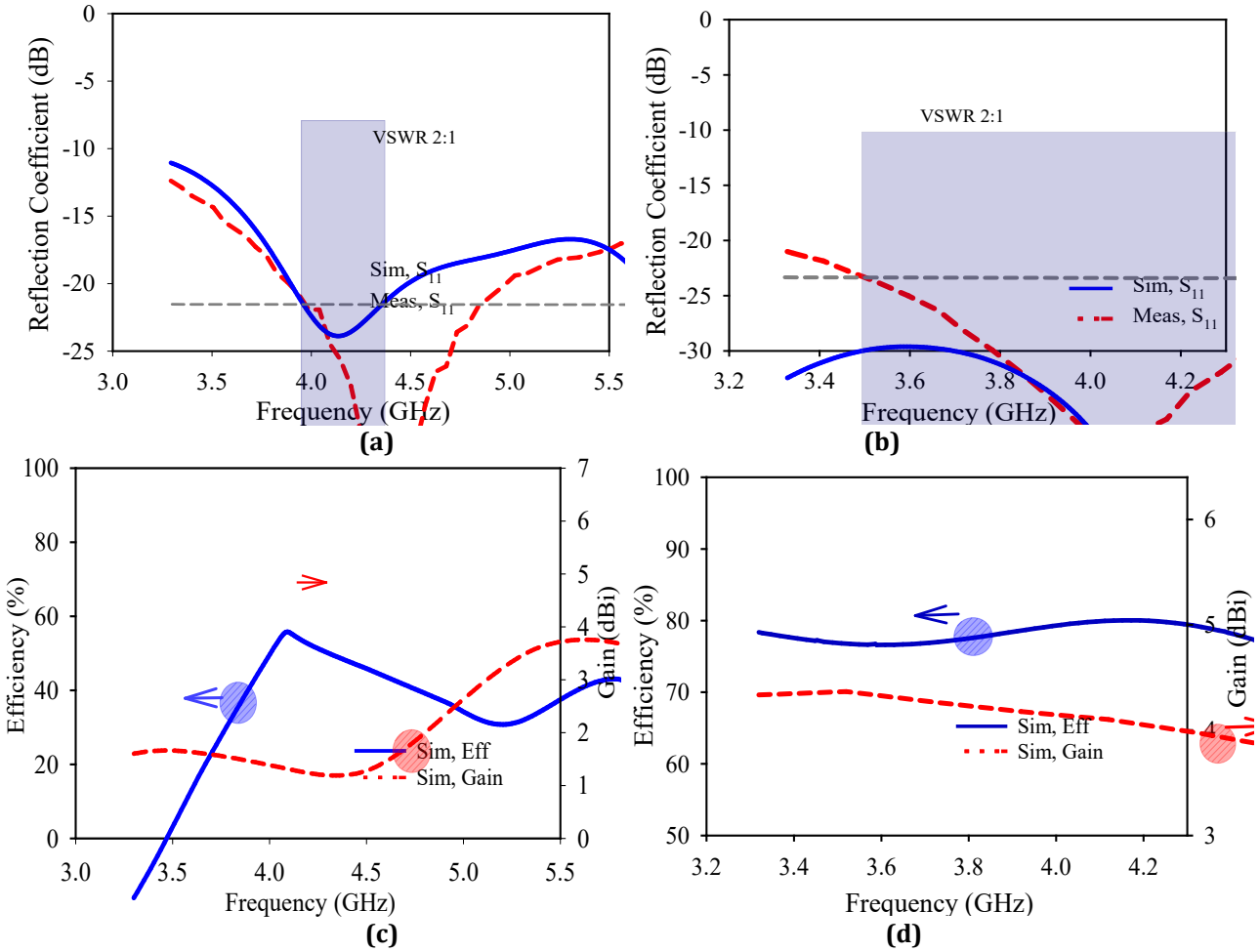

Fig. 8 *Antenna performances in free space, simulated and measured reflection coefficient of (a) dual-ring circular patch antenna; (b) antipodal Vivaldi antenna; simulated efficiency and simulated gain of; (c) dual-ring circular patch antenna; (d) antipodal Vivaldi antenna*

3.2 On-Body Performance of Antipodal Vivaldi Antenna

Figure 9 demonstrates simulated vs measured S_{11} near human body. Due to the antenna's size, placement is limited to the chest and back, as areas such as the shoulder or leg are too small for proper positioning. Additionally, the varying curvature of the human body at different locations (chest, back, arms, legs etc.) necessitate careful consideration of contours to ensure accurate performance evaluation. Since, chest and back are less curvaceous compared to arms or legs, the deformation due to body structure would be less as well if antenna is placed on chest or back.

The reflection coefficient results indicate a frequency shift toward higher frequencies while placing the antenna near body due to electromagnetic impact of antenna. However, the antenna consistently maintained a stable resonance bandwidth of 3.3 GHz to 4.2 GHz in both positions. Since the targeted frequency bands were successfully covered even under on-body conditions, the antenna's performance was deemed satisfactory. Experimental measurements were conducted as well to validate the simulated results. The measured data revealed a frequency shift and a slight reduction in bandwidth, primarily attributed to fabrication and measurement constraints. During the screen-printing process, diffusion between the polyimide and polyester layers altered the antenna's characteristics, impacting its overall performance. Additionally, the lightweight and thin design of the antenna caused a slight tilt in the feedline when connecting the SMA cable during measurements. Given the feedline's critical role in antenna performance, this tilt influenced the resonance frequency. Despite these minor deviations, the antenna demonstrated satisfactory performance, achieving a resonance bandwidth that successfully covers the 5G NR bands of interest: fully covering n48 and nearly covering n77 and n78.

Int. Journal of Integrated Engineering Vol. 17 No. 6 (2025) p. 135-146

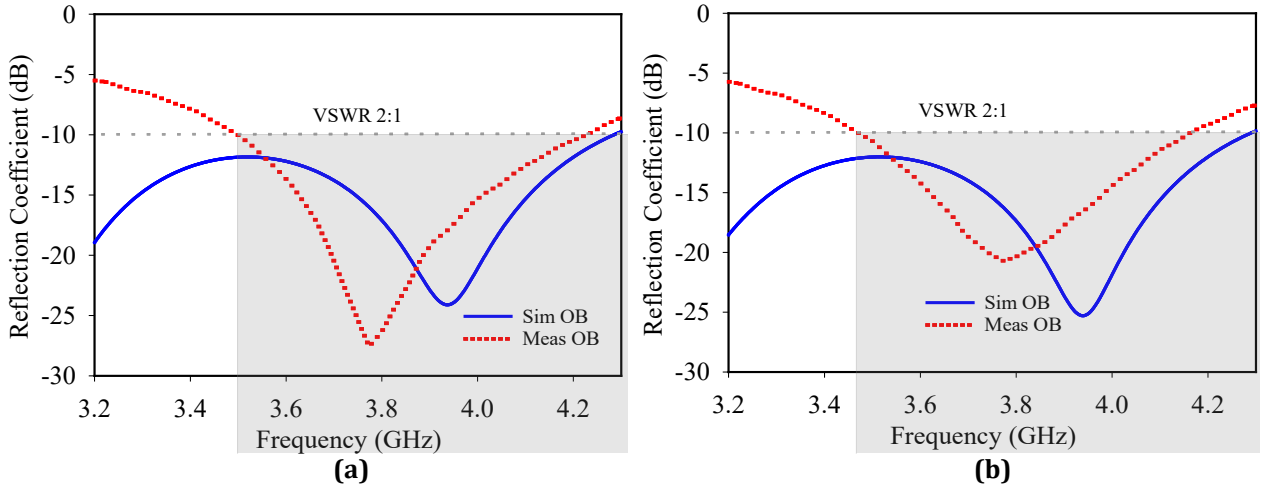

Fig. 9 *Simulated vs measured S_{11} near human body for antipodal Vivaldi antenna, on the (a) back; (b) chest*

3.3 Bending Analysis of Antipodal Vivaldi Antenna

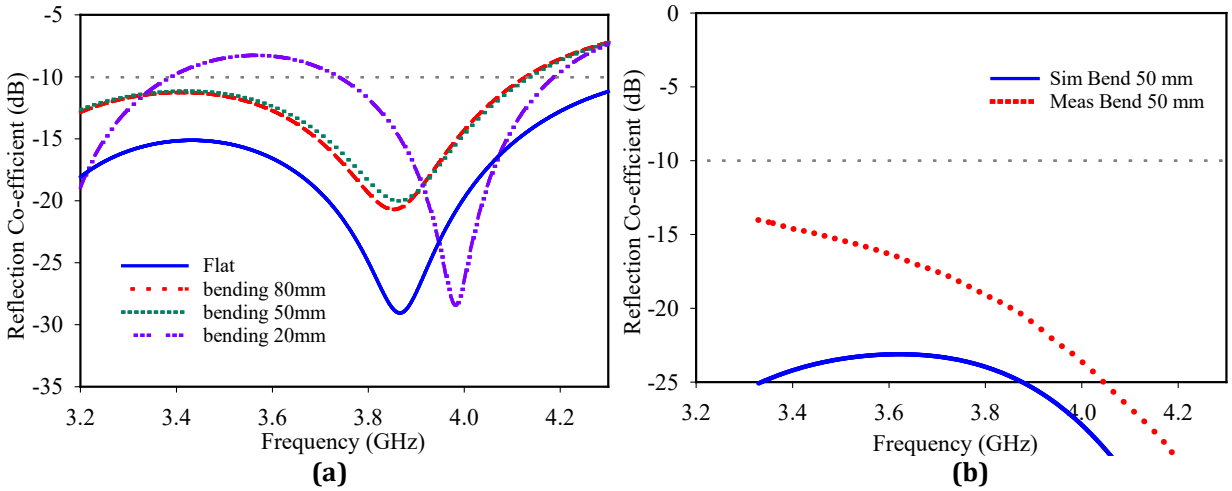

Fig. 10 Bending analysis of antipodal Vivaldi antenna, *S_{11} (a) in different bending conditions in simulation; (b) simulated vs measured in bending radius 50 mm*.

A bending analysis is performed on printed antenna to evaluate its resonance performance under various bending radii, as depicted in Figure 10. Lower bending radius corresponds to a greater bended structure. Achieved results indicate that the antenna maintains satisfactory performance for bending radii down to 50 mm. However, excessive bending, particularly at a radius of 20 mm, leads to significant performance degradation. Therefore, to ensure optimal functionality, a minimum bending radius of 50 mm is recommended. For wearable applications, placement on the chest or back is preferable, as these regions experience minimal structural deformation compared to areas such as the shoulder or arm.

Subsequently, the antenna's bending performance was evaluated through experimental measurements. As shown in Figure 10(b), the measurement results exhibit a strong correlation with the simulation data, following a similar trend. A frequency shift toward higher frequencies was observed, consistent with the previously noted fabrication and measurement constraints encountered in the on-body measurements.

3.4 SAR Analysis of Antipodal Vivaldi Antenna

Specific Absorption Rate (SAR) is assessed for user safety and was evaluated for both chest and back placements at the closest proximity to the body. SAR values are tabulated in Table 4 and the values were computed throughout the bandwidth. An initial input power of 100 mW, as commonly adopted in prior studies, resulted in SAR values exceeding the regulatory limit (2 W/kg) for the back placement. In existing literatures [23], [24], [25] threshold values were proposed. Subsequently, a revised input power threshold of 85 mW was proposed to ensure compliance with safety standards.

Table 4 *Simulated SAR values for antipodal Vivaldi antenna throughout the bandwidth*

Frequency (GHz)	SAR at Back (W/Kg)	SAR at chest (W/Kg)
3.3	1.68	0.98
3.5	1.79	0.84
3.7	1.89	0.92
3.9	1.95	1.00
4.1	1.93	1.05

Table 5 *Comparison of proposed antipodal Vivaldi antenna with previous Vivaldi antenna from literature*

Ref	Substrate	Frequency (GHz)	Size (mm^3)	Gain (dBi)
[26]	Rogers 5880	0.5 to 28	72×40×0.508	-
[27]	Rogers RT5880	23 to 34	16×20×0.807	> 5.65
[28]	Rogers 5880	13 to 20	61×30×0.526	3.1 (max)
[6]	Rogers RT5880	20 to 45	7×10×0.79	6.49 (max)
[29]	Denim jeans	3.7 to 3.85	15×15×0.5	10.7 (max)
Proposed	Polyimide and Polyester	3.3 to 4.2	120×95×0.45	5.42 (max)

The proposed antipodal Vivaldi antenna is compared with previous studies, which predominantly employed rigid or semi-rigid substrates. In contrast, the proposed design utilizes a fully flexible textile substrate. Although this may lead to a slight reduction in bandwidth due to the material properties, it still effectively covers the targeted frequency bands with a sufficient gain performance. Moreover, while similar antipodal antennas on denim fabric have been reported in the literature, the proposed design demonstrates improved resonance bandwidth. Notably, the previously reported denim-based antenna used ShieldIt conductive textile, which has lower durability compared to the screen-printed silver ink used in this work. Although the antenna is relatively large in size, its intended placement on broad areas of the body, such as the chest or back, ensures that the dimensions do not pose any practical limitations or discomfort for the user.

4. Conclusion

This study investigated the fabrication and measurement aspects of a wearable inkjet-printed antenna and compared its performance with that of a conventional copper tape antenna. The alignment between simulated and measured results validated the precision of both the fabrication and measurement processes. Notably, the printed antenna exhibited a broader resonance bandwidth and a closer agreement with simulation results, attributed to its more precise structural integrity. Although the fabrication of the printed antenna is comparatively more expensive, it offers greater durability, which supports long-term performance stability thus the antenna can be used for industrial usage as well. Based on these observations, the printed antenna was found to outperform the copper tape antenna and was selected for further evaluation for wearable application. On-body performance tests were conducted at two body locations, chest and back, demonstrating a consistent resonance bandwidth from 3.3 GHz to 4.2 GHz. These results were comparable to those in free-space conditions, with only minor frequency shifts due to the dielectric properties of the human body. The on-body measurements closely matched the simulations, further confirming effective performance of the antenna in presence of human body. A bending analysis was also carried out to evaluate the robustness of antenna performance to deformation. The antenna exhibited consistent and reliable performance under different bending conditions. Simulation results identified a threshold bending radius of 50 mm, below which the antenna performance began to degrade. To validate this, the antenna was experimentally tested at a 50 mm bending radius, and the measured resonance characteristics closely matched the simulated data, confirming robustness of the design and mechanical flexibility for on-body or curved surface applications. Additionally, specific absorption rate (SAR) analysis was performed in simulation to ensure user safety, and all SAR values remained within the regulatory limit of 2 W/kg across the entire operating bandwidth. These results demonstrate that the printed antenna is a strong candidate for wearable applications.

Future work will include comprehensive performance evaluations, such as measurements of radiation pattern and SAR.

Acknowledgement

The authors would like to acknowledge the financial support provided by Universiti Malaysia Perlis (UniMAP) and Jabil Circuit Sdn. Bhd. through the MTUN Matching 2020 (Batch 2023) Research Grant, under grants number of 9028-00030 and 9002-00156Publisher's Office via Publication Fund E15216.

Conflict of Interest

Authors have no conflict of interests in terms of publishing the paper.

Author Contribution

The authors confirm contribution to the paper as follows: ***study conception and design: Development of the antenna design and application framework*** *was led by Sadia Afroz, Azremi Abdullah Al-Hadi, and Ping Jack Soh;* ***data collection: Experimental data and fabrication process*** *were contributed by Sadia Afroz, Saidatul Norlyana Azemi, Yen San Loh, Lun Hao Tung, Lai Ming Lim, and Zambri Samsudin;* ***analysis and interpretation of results: Antenna performance, simulations, and measurement evaluations*** *were performed by Sadia Afroz, Azremi Abdullah Al-Hadi, Ping Jack Soh, Wee Fwen Hoon, Surentiran Padmanathan, Che Muhammad Nor Che Isa, and Idris Mansor;* ***draft manuscript preparation: Writing and structuring of the manuscript*** *were carried out by Sadia Afroz, Azremi Abdullah Al-Hadi, and Saidatul Norlyana Azemi. All authors reviewed the results and approved the final version of the manuscript.*

References

[1] C. Mendes and C. Peixeiro, "A dual-mode single-band wearable microstrip antenna for body area networks," *IEEE Antennas Wirel. Propag. Lett.*, vol. 16, pp. 3055–3058, 2017, doi: 10.1109/LAWP.2017.2760142.

[2] T. T. Le and T.-Y. Yun, "Wearable Dual-Band High-Gain Low-SAR Antenna for Off-Body Communication," *IEEE Antennas Wirel. Propag. Lett.*, vol. 20, no. 7, pp. 1175–1179, 2021.

[3] H. Li, S. Sun, B. Wang, and F. Wu, "Design of Compact Single-Layer Textile MIMO Antenna for Wearable Applications," *IEEE Trans. Antennas Propag.*, vol. 66, no. 6, pp. 3136–3141, 2018, doi: 10.1109/TAP.2018.2811844.

[4] C. Hertleer, A. Tronquo, H. Rogier, and L. Van Langenhove, "The Use of Textile Materials to Design Wearable Microstrip Patch Antennas," *Text. Res. J.*, vol. 78, no. 8, pp. 651–658, 2008, doi: 10.1177/0040517507083726.

[5] S. Afroz, A. A. Al-hadi, S. N. Azemi, and W. F. Hoon, "Dual Band Circular Patch Flexible Wearable Antenna Design for Sub-6 GHz 5G Applications," in *2022 IEEE International RF and Microwave Conference (RFM) 2022*, Kuala Lumpur, Malaysia: IEEE, 2022, pp. 22–25. doi: 10.1109/RFM56185.2022.10065238.

[6] M. B. Lakshmi, K. K. Srinivas, D. J. Devi, M. Bhargavi, and M. J. Moses, "Design and Analysis of Compact Millimeter-Wave Vivaldi Antenna for Wearable WBAN Application," in *2025 8th International Conference on Electronics, Materials Engineering & Nano-Technology (IEMENTech)*, IEEE, 2025, pp. 1–6. doi: 10.1109/IEMENTech65115.2025.10959656.

[7] S. S. Modasiya and B. J. Makwana, "A Novel Radial Corrugated Vivaldi Antenna for UWB Applications and Enhanced Gain," vol. 6, no. July, pp. 813–824, 2025, doi: 10.47857/irjms.2025.v06i03.04130.

[8] S. B. Roshni, M. P. Jayakrishnan, P. Mohanan, and K. P. Surendran, "Design and fabrication of an E-shaped wearable textile antenna on PVB-coated hydrophobic polyester fabric," *Smart Mater. Struct.*, vol. 26, no. 10, 2017, doi: 10.1088/1361-665X/aa7c40.

[9] R. Aprilliyani, P. A. Dzagbletey, J. H. Lee, M. J. Jang, J. H. So, and J. Y. Chung, "Effects of Textile Weaving and Finishing Processes on Textile-Based Wearable Patch Antennas," *IEEE Access*, vol. 8, pp. 63295–63301, 2020, doi: 10.1109/ACCESS.2020.2984934.

[10] S. Afroz, A. A. Al-hadi, S. N. Azemi, and W. F. Hoon, "A 3.5 GHz Wearable Antipodal Vivaldi Antenna for 5G Applications," *2023 IEEE Int. Symp. Antennas Propag.*, vol. 4, no. c, pp. 1–2, 2023, doi: 10.1109/ISAP57493.2023.10388737.

[11] U. Ali, S. Ullah, A. Basir, B. Kamal, L. Matekovits, and H. Yoo, "Design and SAR Analysis of AMC-Based Fabric Antenna for Body-Centric Communication," *IEEE Access*, vol. 11, no. June, pp. 73894–73911, 2023, doi: 10.1109/ACCESS.2023.3295993.

[12] S. Sankaralingam, S. Dhar, and B. Gupta, "Performance of Fully Fabric Wearable Circular Patch Antennas in the Vicinity of Human Body at 2.45 GHz," in *"2013 International Symposium on Electromagnetic Theory,"* IEEE, 2013, pp. 179–184. doi: 10.1016/j.proeng.2013.09.089.

[13] N. I. Zaidi *et al.*, "Analysis on Bending Performance of the Electro-Textile Antennas with Bandwidth Enhancement for Wearable Tracking Application," *IEEE Access*, vol. 10, pp. 31800–31820, 2022, doi: 10.1109/ACCESS.2022.3160825.

[14] K. N. Paracha, S. K. Abdul Rahim, P. J. Soh, and M. Khalily, "Wearable Antennas: A Review of Materials, Structures, and Innovative Features for Autonomous Communication and Sensing," *IEEE Access*, vol. 7, pp. 56694–56712, 2019, doi: 10.1109/ACCESS.2019.2909146.

[15] A. A. Althuwayb *et al.*, "Metasurface-Inspired Flexible Wearable MIMO Antenna Array for Wireless Body Area Network Applications and Biomedical Telemetry Devices," *IEEE Access*, vol. 11, no. January, pp. 1039–1056, 2023, doi: 10.1109/ACCESS.2022.3233388.

[16] M. El Gharbi, R. Fernández-García, and I. Gil, "Embroidered wearable Antenna-based sensor for Real-Time breath monitoring," *Meas. J. Int. Meas. Confed.*, vol. 195, no. February, 2022, doi: 10.1016/j.measurement.2022.111080.

[17] P. M. Potey and K. Tuckley, "Design of wearable textile antenna for low back radiation," *J. Electromagn. Waves Appl.*, vol. 34, no. 2, pp. 235–245, 2020, doi: 10.1080/09205071.2019.1699170.

[18] A. Ahmad, F. Faisal, S. Ullah, and D. Y. Choi, "Design and SAR Analysis of a Dual Band Wearable Antenna for WLAN Applications," *Appl. Sci.*, vol. 12, no. 18, 2022, doi: 10.3390/app12189218.

[19] U. Ali, S. Ullah, M. Shafi, S. A. A. Shah, I. A. Shah, and J. A. Flint, "Design and comparative analysis of conventional and metamaterial-based textile antennas for wearable applications," *Int. J. Numer. Model. Electron. Networks, Devices Fields*, vol. 32, no. 6, pp. 1–17, 2019, doi: 10.1002/jnm.2567.

[20] S. Arulmurugan, S. T. R. Kumar, J. Siden, and Z. C. Alex, "Circular Polarized Dual-Band Wearable Screen-Printed MIMO Antenna Integrated With AMC for WBAN Communications," *IEEE Open J. Antennas Propag.*, vol. 5, no. 6, pp. 1805–1814, 2024, doi: 10.1109/OJAP.2024.3458968.

[21] H. Lei, T. Patel, J. Lopez, and J. D. Mackenzie, "Screen Printed Flexible Antennas for 24 GHz ISM band and mmWave Applications," *IEEE J. Flex. Electron.*, vol. PP, pp. 1–9, 2025, doi: 10.1109/JFLEX.2025.3560936.

[22] M. Sharma *et al.*, "Miniaturized Quad-Port Conformal Multi-Band (QPC-MB) MIMO Antenna for On-Body Wireless Systems in Microwave-Millimeter Bands," *IEEE Access*, vol. 11, no. September, pp. 105982–105999, 2023, doi: 10.1109/ACCESS.2023.3318313.

[23] S. Kumar *et al.*, "Wideband Circularly Polarized Textile MIMO Antenna for Wearable Applications," *IEEE Access*, vol. 9, pp. 108601–108613, 2021, doi: 10.1109/ACCESS.2021.3101441.

[24] amor Smida, amjad Iqbal, abdullah J. alazemi, M. I. Waly, R. Ghayoula, and S. Kim, "Wideband Wearable antenna for Biomedical Telemetry applications," *IEEE Access*, vol. 8, pp. 15687–15694, 2020, doi: 10.1109/aCCESS.2020.2967413.

[25] Z. Zhao *et al.*, "A Miniaturized Wearable Antenna With Five Band-Notched Characteristics for Medical Applications," *IEEE Antennas Wirel. Propag. Lett.*, vol. 22, no. 6, pp. 1246–1250, 2023, doi: 10.1109/LAWP.2023.3237714.

[26] J. Li, H. Zhai, and M. Wang, "A Compact Vivaldi Antenna with Enhanced Bandwidth and Mismatch Suppression," *IEEE Trans. Antennas Propag.*, vol. 73, no. 1, pp. 623–628, 2024, doi: 10.1109/TAP.2024.3496083.

[27] J. Ahmad, M. Hashmi, A. Bakytbekov, and F. Falcone, "Design and Analysis of a Low Profile Millimeter-Wave Band Vivaldi MIMO Antenna for Wearable WBAN Applications," *IEEE Access*, vol. 12, no. April, pp. 70420–70433, 2024, doi: 10.1109/ACCESS.2024.3401865.

[28] B. Liu, Y. Zhang, J. Lin, J. Zhuo, K. Lai, and L. Ye, "Endfire Gain Enhancement Enabled by a Modified Antipodal Vivaldi Antenna with Metamaterials," *IEEE Photonics Technol. Lett.*, vol. 36, no. 23, pp. 1385–1388, 2024, doi: 10.1109/LPT.2024.3480324.

[29] A. R. H. Alhawari *et al.*, "Wearable metamaterial dual-polarized high isolation uwb mimo vivaldi antenna for 5g and satellite communications," *Micromachines*, vol. 12, no. 12, pp. 1–31, 2021, doi: 10.3390/mi12121559.